Comprehensive analysis of TESS Full Orbital Phase Curve of WASP-121b

Mohammad Eftekhar[1]

[1] *Department of Physics, Faculty of Science, University of Zanjan, Iran.*

Abstract

We present the full phase curve analysis of the ultrahot Jupiter WASP-121b ($R_p \simeq 1.865 R_J$, $M_p \simeq 1.184 M_J$) using observations from the Transiting Exoplanet Survey Satellite (TESS). Our comprehensive phase curve model includes primary transit, secondary eclipse, thermal emission, reflection, and ellipsoidal tidal distortion, which are jointly fit to extract the information of all parameters simultaneously from the data sets. We also evaluated and calculated the amplitude of Doppler beaming to be ~ 2 ppm, but given the precision of the photometric data, we found it to be insignificant. After removing the instrumental systematic noise, we reliably detect the secondary eclipse with a depth of 489^{+16}_{-10} parts-per-million (ppm), dominated by thermal emission. Using the TESS bandpass, we measure the dayside $2941^{+61}_{-150}K$ and nightside $2236^{+38}_{-97}K$ temperatures of WASP-121b. We find that a hotspot is well aligned with the substellar point, leading to the conclusion that there is an inefficient heat distribution from the dayside to the nightside. Our estimated geometric albedo, $A_g = 0.069^{+0.06}_{-0.02}$, suggest that WASP-121b has a low geometric albedo. Finally, our estimated amplitude of the ellipsoidal variation signal is in agreement with the predictions of the theoretical expectations.

Phase curve

In addition to the primary transit light curve and secondary eclipse (Kreidberg 2015), photometric observations reveal additional variation induced by the orbiting exoplanet over the full planetary orbit. This variation can be decomposed into several components, namely:

Thermal emission

In order to model WASP-121b's thermal emission component, we used a semi-physical model based on Zhang Showman (2017) which has been implemented in `spiderman` (Louden Kreidberg 2018).

Reflected light

A basic form of reflection phase modulation can be described as (Shporer 2017):

$$Reflection = A_{ref}(1+\cos(2\pi(\phi+\Delta_P/P)+\pi)) \quad (1)$$

where, A_{ref} is the amplitude of the reflection, which depends on the albedo, ϕ, is the orbital phase, P is the orbital period, and Δ_P is the phase shift.

Doppler beaming

The amplitude of the beaming component, A_D, can be computed using the physical parameters of the system as (Shporer 2017):

$$A_D = 0.0028\alpha_D(\frac{P}{day})^{-1/3}\times(\frac{M_1+M_2}{M_\odot})^{-2/3}(\frac{M_2 \sin i}{M_\odot}) \quad (2)$$

Here M_1, M_2, $M_\odot$ are the masses of the host star, planet, and sun, respectively. i is the orbital inclination angle.

We ignore the Doppler beaming because we estimate the amplitude of Doppler beaming to be ~ 2 ppm, which is significantly smaller than the precision achievable by TESS.

Ellipsoidal variation

The gravitational pull of a close-in exoplanet causes the host star to deviate from a spherical form to an ellipsoid. This deformation produces photometric orbital modulations with an amplitude that can be approximated by Shporer (2017)

$$Ellipsoidial = A_{ellip}(1+\cos(4\pi\phi-\pi)) \quad (3)$$

Acknowledgements

We used the publicly available data from the Mikulski Archive for Space Telescopes (MAST). Funding for the TESS mission is provided by NASA's Science Mission directorate.

Observations

Although the dominant systematics were corrected by default in the PDCSAP light curve, we corrected it further for the remaining systematics. To do this, we used the median detrending algorithm with a window length of one orbital period to smooth the PDCSAP light curve and keeping variability at the planetary period. the regression was implemented using the Python package `wotan` (Hippke et al. 2019).

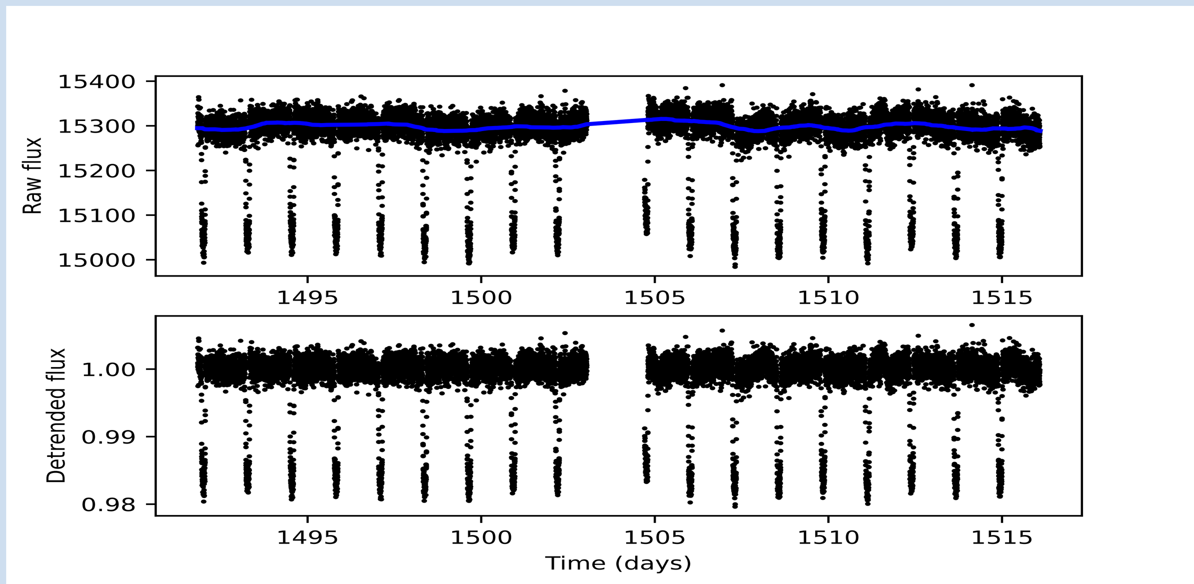

Figure 1. (Top) The PDCSAP photometry is indicated with black dots, and the solid blue line shows the trend obtained by `wotan`. (Bottom) PDCSAP light curve after deterending and normalization by its median.

Model and Fitting procedure and Results

The best fit parameters and their associated uncertainties are determined using a Markov Chain Monte Carlo (MCMC) approach using the affine invariant ensemble sampler emcee package (Foreman-Mackey et al. 2013).

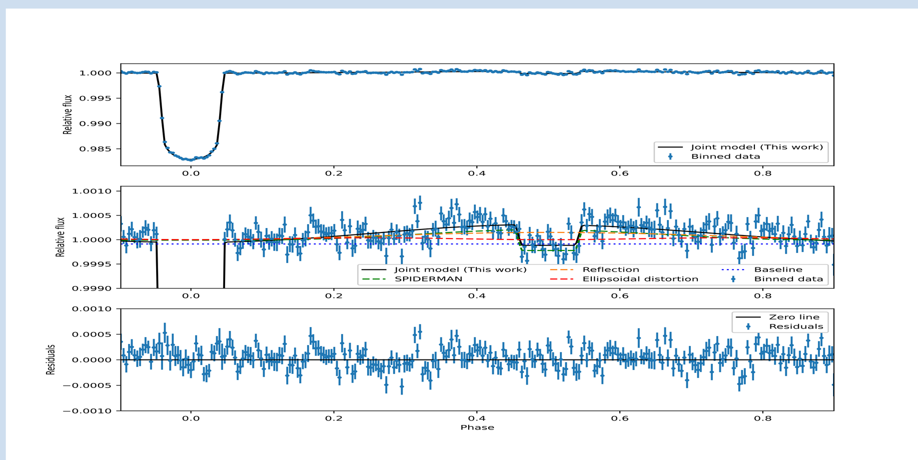

Figure 2.(Top) Our reprocessed data of WASP-121 (blue dots) and best fitted model (black curve). (Middle) zoom of the secondary eclipse. (Bottom) The best fitted model's corresponding residuals.

Parameter	Value	(Bourrier et al.2020)	(Daylan et al.2021)
R_p/R_s	$0.1234^{+0.0005}_{-0.0005}$	$0.12355^{+0.00029}_{-0.00033}$	$0.12488^{+0.00072}_{-0.00072}$
a/R_s	$3.792^{+0.023}_{-0.039}$	$3.8216^{+0.0074}_{-0.0087}$	$3.674^{+0.035}_{-0.035}$
i (deg)	$88.80^{+1.27}_{-1.23}$	$89.10^{+0.68}_{-0.58}$	
u_1	$0.260^{+0.034}_{-0.042}$	$0.268^{+0.039}_{-0.039}$	$0.285^{+0.058}_{-0.058}$
u_2	$0.132^{+0.056}_{-0.082}$	$0.138^{+0.075}_{-0.076}$	$0.06^{+0.11}_{-0.11}$
ξ	$-0.022^{+0.159}_{-0.141}$	$-0.016^{+0.061}_{-0.064}$	
T_N (K)	2236^{+97}_{-38}	2190^{+145}_{-106}	2022^{+202}_{-652}
ΔT_{DN} (K)	734^{+28}_{-55}	710^{+145}_{-106}	1010^{+202}_{-652}
Baseline	$-0.00014^{+1.7\times10^{-6}}_{-0.8\times10^{-6}}$		
Eclipse depth (ppm)	489^{+16}_{-10}	419^{+47}_{-42}	482^{+41}_{-39}
A_{ref} (ppm)	$73^{+2.2}_{-3.1}$		
Δ_P	$-0.0008^{+0.0012}_{-0.0071}$		
A_{ellip} (ppm)	20^{+2}_{-3}		8^{+6}_{-12}

CHEOPS Science Workshop VI — Mohammad Eftekhar 16 / 17

Figure 4. Our the best fitted values with comparison with Daylan et al. (2021), and Bourrier et al. (2020)

Conclusion

The most remarkable result of our study is the simultaneous measurement of the primary transit, the secondary eclipse (he most precise estimate for WASP-121b to date), and the robust detection of the total phase curve component corresponding to thermal emission, reflected light, and ellipsoidal variation.

References

Hippke, M., David, T. J., Mulders, G. D., Heller, R. 2019, AJ, 158, 143

Kreidberg, L. 2015, Publications of the Astronomical Society of the Pacific, 127,116

Zhang, X. Showman, A. P. 2017, ApJ, 836, 73

Louden, T. Kreidberg, L. 2018, MNRAS, 477, 2613

Shporer, A. 2017, PASP, 129, 072001

Foreman-Mackey, D., Hogg, D. W., Lang, D., Goodman, J. 2013, PASP, 125, 306

Bourrier, V., Ehrenreich, D., Lendl, M., 2020, AA, 635, A205

Daylan, T., G unther, M. N.,2021, AJ, 161, 131